Predicted High-Temperature Superconductivity in Rare Earth Hydride ErH_2 at Moderate Pressure

Yiding Liu(刘一丁)[1,2], Qiang Fan(范强)[3], Jianhui Yang(杨建会)[1], Lili Wang(王丽丽)[4], Weibin Zhang(张伟斌)[5], and Gang Yao(姚钢)[6,7*]

[1]*College of Mathematics and Physics, Leshan Normal University, Leshan 614004, China*
[2]*Institute of Atomic and Molecular Physics, Sichuan University, Chengdu 610065, China*
[3]*School of New Energy Materials and Chemistry, Leshan Normal University, Leshan 614004, China*
[4]*Institute of Computer Application, China Academy of Engineering Physics, Mianyang 621900, China*
[5]*College of Physics and Electronics Information, Yunnan Key Laboratory of Optoelectronic Information Technology, Yunnan Normal University, Kunming 650500, China*
[6]*School of Physical Science and Technology, Southwest University, Chongqing 400715, China*
[7]*Tsung-Dao Lee Institute, Shanghai Jiao Tong University, Shanghai 200240, China*

(Received 18 September 2022; accepted manuscript online 23 November 2022)

Hydrides offer an opportunity to study high critical temperature (high-T_c) superconductivity at experimentally achievable pressures. However, the pressure needed remains extremely high. Using density functional theory calculations, herein we demonstrate that a new rare earth hydride ErH_2 could be superconducting with $T_c \sim 80$ K at 14.5 GPa, the lowest reported value for compressed hydrides to date. Intriguingly, due to Kondo destruction, superconductivity was prone to exist at 15 GPa. We also reveal an energy gap at 20 GPa on the background of normal metallic states. At 20 GPa, this compressed system could act as a host of superconductor judged from a sharp jump of spontaneous magnetic susceptibility with an evanescent spin density of state at Fermi level. Finally, electron pairing glue for ErH_2 at these three typical pressures was attributed to the antiferromagnetic spin fluctuation.

DOI: 10.1088/0256-307X/39/12/127403

Hydrogen in certain hydrides can become metallic at a lower pressure than pure hydrogen, presumably because of additive effects from chemical precompression.[1] These hydrides may be well superconducting up to high critical transition temperature (high-T_c). Several theoretical and experimental efforts were underway to better understand the high-T_c superconductivity of such hydrides. These compounds include GeH_4 (64 K at 220 GPa),[2] YH_3 (40 K at 17.7 GPa),[3] H_3S (203 K at 90 GPa),[4] VH_8 (71.4 K at 200 GPa),[5] LaH_{10} (274–286 K at 210 GPa,[6] 260 K at 180–200 GPa,[7] and 250 K at 170 GPa[8]), YbH_6 (145 K at 70 GPa), TmH_6 (25 K at 50 GPa),[9] LuH_6 (273 K at 100 GPa),[9] and other room-temperature superconductors YH_{10} (305–326 K at 250 GPa,[6] 303 K at 400 GPa[10]), Li_2MgH_{16} (473 K at 250 GPa).[11] Note that in all the above-mentioned hydrides, the major glue for electron pairing is phonon.

Among rare-earth metals, Er showed a powerful getter for hydrogen.[12] The stoichiometry erbium dihydride (ErH_2) and its nonstoichiometric composition ErH_{2+x} ($-0.15 < x < 0.15$) both crystallize with fcc-CaF_2 type crystal structure (space group: $Fm\bar{3}m$), which has often been described as the β-phase.[13,14] It should be noted that the existence of ErH_3 has been predicated and confirmed before, however, no superconductivity was observed.[15,16] Hence, in the following discussion, we focus on ErH_2. The conventional unit cell of ErH_2 is displayed in Fig. 1, in which the H atoms occupied the tetrahedral sites of the Er fcc lattice. In the meantime, the f electrons in lattice are often neither fully localized around their host nuclei nor fully itinerant. This localized versus itinerant duality has proposed the involvement of f electrons as valence ones in the systems, that is, strongly correlated-electron materials, therefore promoting the emerging researches of heavy fermion superconductors.[17] On the other hand, it was argued that antiferromagnetic (AFM) spin fluctuation was another plausible pairing mechanism driven by Coulomb repulsion in this system, and could lead to high-T_c superconductivity.[18–21] The Hubbard model could be consequently applied to this system.[22–24] AFM spin fluctuation could be reflected with mutation from a large Fermi surface (FS) to a small one,[25] and a jump of spin DOS at Fermi level (E_F) or spontaneous magnetic susceptibility (χ_s).[19,21] One central issue that naturally arises is whether a compressed system can be superconducting, and if there is another pairing mechanism for it. Despite the investigation discussed above for f electrons in a crystal, a systematic study of possible pressure-induced superconductivity in ErH_2 is still missing.

In this work, by using first-principles calculations, we reveal that the heavy fermion hydride ErH_2 is a superconductor with high-T_c at much lower pressure. In particular, traces for several accompanying physical behaviors, including FS nesting, Kondo effect, Kondo destruction, and energy gap on the background of normal metallic states, are reported.

*Corresponding author. Email: yaogang@swu.edu.cn
© 2022 Chinese Physical Society and IOP Publishing Ltd

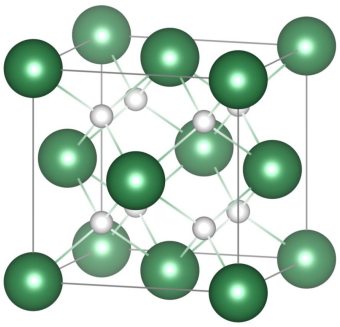

Fig. 1. A unit cell of ErH_2 crystal is displayed. The larger green atoms represent the erbium fcc lattice. The eight smaller grey atoms represent hydrogen occupying all of the tetrahedral sites.

Our spin-polarized calculations based on the density functional theory (DFT) were performed using the Cambridge serial total energy package (CASTEP) code.[26] The exchange and correlation interactions were described by the generalized gradient approximation (GGA) of Perdew and Wang (PW91).[27] Norm-conserving pseudopotentials were used to describe the properties of the perfect crystal. The valence electron configurations for Er and H were $4f^{11}5d^15s^25p^66s^2$ and $1s^1$, respectively. The energy cutoff was set to be 380 eV. For the geometry optimizations of the shape and size of the cell, the Brillouin zone integration was performed using a $10 \times 10 \times 10$ Monkhorst–Pack k-points mesh, and for electronic structure calculations including FSs and electron localization functions (ELFs), a dense mesh with $36 \times 36 \times 36$ k-points was used. All above parameter settings were verifiable to convergence tests. In addition, the Er-f states were treated employing the GGA + U approach[23] with $U = 6$ eV, as suggested in the relevant previous reports.[28] The phonon calculations were performed using finite displacements method.[29]

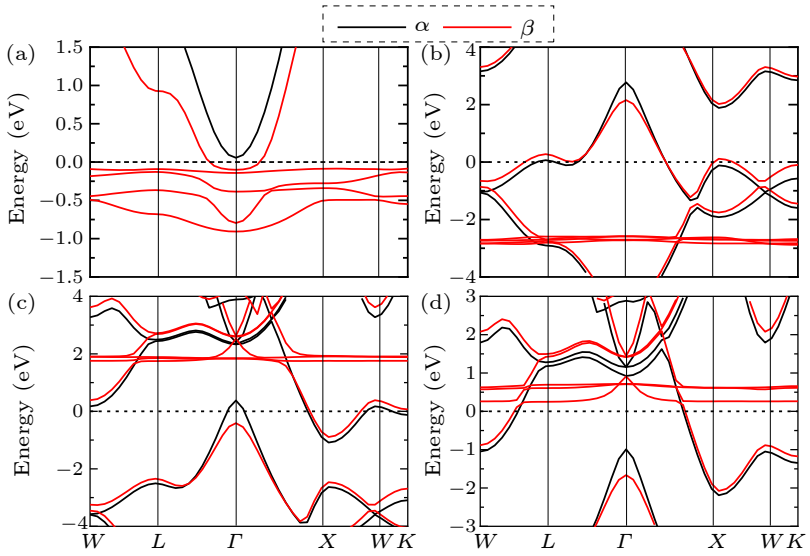

Fig. 2. Band structures of ErH_2 under ambient pressures ranging from 0 to 21.5 GPa: (a) 0 GPa, (b) 14.5 GPa, (c) 15 GPa, and (d) 0.5 GPa. At the rest of this pressure range except 20 GPa, band structures are similar with (d), α and β denote spin-up and spin-down, respectively.

ErH_2 possesses AFM[30] that is subjected to have an intimate link with both FS nesting[31] and superconductivity.[19] Firstly, the FS topologies, electronic density of states (DOS) and band structures were calculated at ambient pressures ranging from 0 to 21.5 GPa. Figure 2 shows the band structures under 0, 14.5, 15 GPa and other pressures except 20 GPa. As shown in Fig. 3, there are three types in topology, electron-like type under 0 GPa, hole-like type at 14.5 and 15 GPa (large and small respectively), and open type at other pressures except for 20 GPa under which DOS and band structure revealed a gap, thus showed no FS around its E_F. Compared with 0 GPa, at which the corrugated FS reflected the influence of phonon on the properties of electrons around E_F, the other smooth FSs indicated that the interaction between phonon and electrons decreased considerably.[32]

Figure 3(b) shows the topology of the hole-like-FS at 14.5 GPa. It did show nesting property in accordance with its AFM.[30] This consistency between FS nesting and AFM had also been confirmed in $ErGa_3$.[31] This FS at 14.5 GPa is apparently the largest one in the whole applied pressures. As shown in Fig. 4(c), in the conduction band region at this pressure, there is a sharp spin-down $f(\beta)$ peak in the range 4–5 eV just corresponding to the spin-up conduction d (α) electrons in this energy range. Moreover, the itinerancy of these f electrons could be embodied with the localized s electrons of H in the ELF at this pressure [Fig. 4(a)]. Compared with the ELFs under other pressures [Fig. 4(b)] where electrons localized around Er, the ELF at 14.5 GPa [Fig. 4(a)] showed a distinct localization of electrons around H. Judging from Fig. 4(c) in which two large H-derived sharp s-electron DOS peaks [spin-up (α) and spin-down (β) respectively] were most adjacent to the E_F, H atoms were essentially isolated like atomic H in this lattice. Hence, the result at 14.5 GPa could infer the Kondo effect.[17] The fully itinerant $f(\beta)$ electrons like magnetons immersed in conduction $d(\alpha)$ electrons, entangled with them sufficiently and contributed to the Fermi

volume.[17,33] Accordingly, the full formation of a large FS could correspond to heavy fermion superconductivity.[25] We show in Fig. 4(e) the variation of spin DOS at E_F and χ_s along with the applied pressures. Combining with the explicit hopping of spin DOS at E_F at 14.5 GPa without abrupt jump of χ_s and the largest FS with its nesting [Fig. 3(b)], superconductivity could be implied at 14.5 GPa being mediated by AFM spin fluctuation.[18–21]

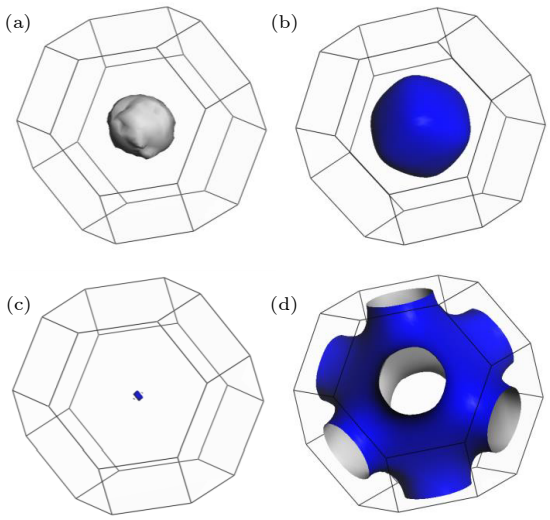

Fig. 3. Types of FSs for ErH_2 at ambient pressures ranging from 0 to 21.5 GPa: (a) electron-like type under 0 GPa, [(b), (c)] hole-like type at 14.5 and 15 GPa, respectively, (d) open type at 0.5 GPa. At the rest of this pressure range except 20 GPa, the FSs are of open type similar with the one at 0.5 GPa.

Fermi liquid (FL) could easily exist in this state.[17] Furthermore, based on phonon calculation, the lattice specific heat at 14.5 GPa was also calculated out.[34] The specific heat C in the form of C/T dependence on T^2, as shown in Fig. 5 under ambient pressures, was obtained with the formula[35,36]

$$C = \gamma_1 T^3 + \gamma_2 T. \tag{1}$$

Here, the first term represents the lattice specific heat, the second term denotes the electrons contribution, γ_1 is interatomic force constant, $\gamma_2 = \frac{\pi^2}{3} k_B^2 g(E_F)$ with k_B being Boltzmann's constant, and $g(E_F)$ is the DOS at E_F. For the FL state, the electron specific heat depends on T linearly, i.e., $\gamma_2 T$. In other words, T_c could be obtained by locating the kink point of the C/T versus T^2 plot for the superconducting transition.[32] With these regards, the T_c of ErH_2 at 14.5 GPa is found to be 78.9 K from the simulated $C(T)$ curve shown in Fig. 5. Note that this T_c value is around boiling point of liquid nitrogen.

In contrast to the Kondo effect, superconductivity could also be driven by Kondo destruction transforming from a large FS to a small one in heavy fermion superconductors, such as $CeCu_2Si_2$.[25] The FS of ErH_2 at 15 GPa collapsed abruptly as shown in Fig. 3(c), which was identified as destruction of Kondo effect.[17,25,37] Hence, this quantum criticality at 15 GPa could also be prone to possess superconductivity. This phenomenon implied the fully localization of f electrons around their host nuclei, i.e., Er, as the ELF shown in Fig. 4(b). The fact that the localized f electrons do not contribute to the Fermi volume[17,33] was consistent with the small FS [Fig. 3(c)].

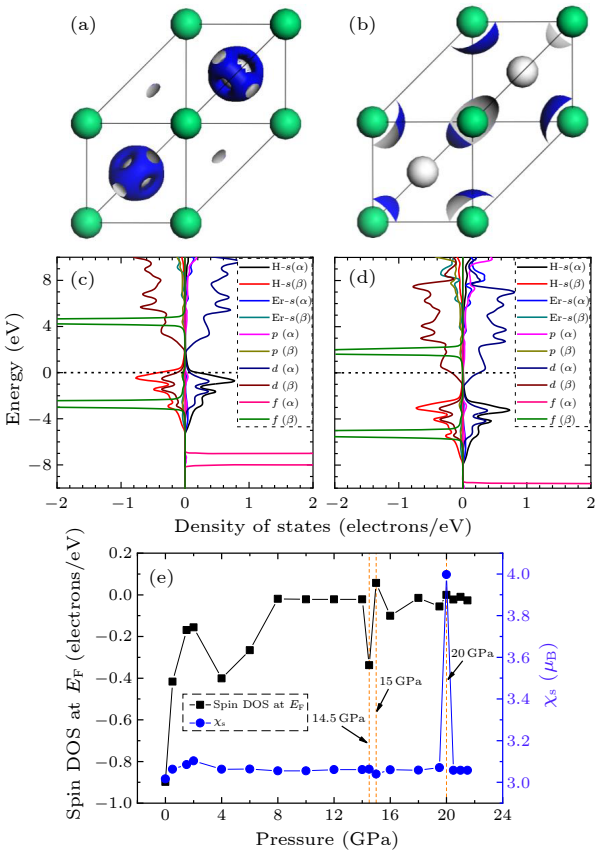

Fig. 4. (a) Schematic diagram of electron localization function (ELF) at 14.5 GPa. (b) The ELFs under other pressures of the whole applied pressures. The primitive cell of ErH_2 crystal is displayed. Green spheres represented Er, while grey spheres represented H. [(c), (d)] The DOS at 14.5 and 15 GPa, respectively. (e) The variation of spin DOS at E_F and the spontaneous magnetic susceptibility (χ_s) along with the applied pressures.

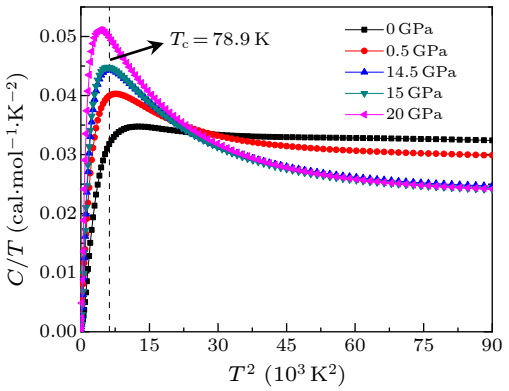

Fig. 5. T^2 dependence of the specific heat in the form of C/T under ambient pressures for ErH_2.

Subsequently, with the Kondo destruction [Fig. 3(c)], the Ruderman–Kittel–Kasuya–Yosida (RKKY) interaction played a dominant role that led to the crossover fea-

ture from FL at 14.5 GPa to non-fermi-liquid (NFL) behavior at 15 GPa, where the indirect interaction among the localized f electrons with magnetic moments was mediated mainly by the conduction d electrons.[17,25] The DOS is shown in Fig. 4(d). Therefore, despite the superconductivity as predicted at 15 GPa, the dependence of electrons specific heat on T is nonlinear,[35,36] so the T_c value at 15 GPa could not be obtained from the kink point of the C/T versus T^2 curve in Fig. 5. This superconductivity could also be inferred with the medium of AFM spin fluctuation from the noticeable hopping of spin DOS at E_F between 14.5 and 15 GPa without steep variation of χ_s in this pressure region [Fig. 4(e)] as well as this FS jump.[18–21] The accompanying behaviors, which could also to some extent support the affirmation of superconductivity at 15 GPa, are presented in the Supplemental Material.[38]

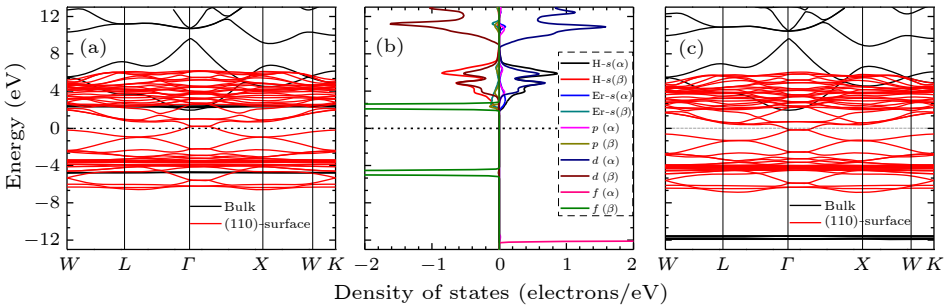

Fig. 6. [(a), (c)] The band structures of this bulk at 20 GPa with electronic spin-down and spin-up, respectively. The band structures of (110) surface built with $1 \times 2 \times 1$ supercell of this bulk at 20 GPa are also plotted with red color in (a) and (c). The energy scales of this metallic surface state are from -6 to 6 eV. (b) The DOS of this bulk at 20 GPa. Here, α and β denote spin-up and spin-down, respectively.

From the spin-polarized DOS and band structures of ErH_2 at 20 GPa [Figs. 6(a)–6(c)], an energy gap of 6.6 eV can be observed on the background of normal metallic states under the rest of applied pressures. The itinerant electrons were from s electrons of H and s, p, d ones of Er, whose all spins with up and down directions had almost the same weight and symmetric distribution. The fully localized electrons were from f electrons of Er as shown in the ELF [Fig. 4(b)] and the DOS [Fig. 6(b)]. This manifested that itinerant AFM at 20 GPa vanished abruptly, leading to a localized AFM insulating state.[39] This transition results in a sharp jump in χ_s and an evanescent spin DOS at E_F [Fig. 4(e)], which could also signify an AFM spin fluctuation.[18–21] Therefore, ErH_2 at this pressure could act as a host of superconductor owing to this pairing glue.[18–21] This implication is supported by the competition between spin density wave (SDW) and superconductivity.[17,39–41] The existence of SDW could be determined with Pauli paramagnetic susceptibility, $\chi_P(0)$, which was expressed as follows:[39]

$$\chi_P(0) = 2\mu_B^2 \mu_0 g(E_F), \tag{2}$$

where μ_B is Bohr magneton, μ_0 is vacuum permeability and $g(E_F)$ is the DOS at E_F. The SDW is suppressed from the zero DOS at E_F [Fig. 6(b)] and Eq. (2). This hypothesis could also be supported by the tiny and clear deviation of the V/V_0 versus pressures relation calculated directly with DFT at this pressure away from the monotonous trend of the curve fitted with E–V data of this work (see Fig. S1 in the Supplemental Material[38]). The hybridization between localized f moments and itinerant electrons is very weak at this pressure, implying the NFL behavior. Meanwhile, as shown in Figs. 6(a) and 6(c), the band structures of (110) surface of this bulk at 20 GPa in the range from -6 to 6 eV exhibiting metallic, come within the gap of this bulk. This metallic surface state with bulk insulating state emerged also in the archetype Kondo insulator, i.e., SmB_6.[37] Our results could postulate a possibility for topological superconductor which could host Majorana zero mode.[42,43]

Note that the ErH_2 under 0, 14.5, 15 and 20 GPa are dynamically stable as no imaginary phonon mode is observed (see Fig. S3 in the Supplemental Material[38]).

To summarize, we have revealed superconductivity that emerged in ErH_2 under moderate pressures 14.5, 15 and 20 GPa by using DFT calculations. It is proposed that ErH_2 at 14.5 GPa is a potential high-T_c superconductor with $T_c \sim 80$ K. The gapped bulk state with metallic surface state at 20 GPa could be conducive to the exploration of topological superconductor, which will stimulate further experimental and theoretical studies for the feasibility of ErH_2 to host Majorana zero mode.

Acknowledgements. This work was supported by the National Natural Science Foundation of China (Grant No. 12104294), and the Research Project of Leshan Normal University (Grant No. 801/204190415). This work was carried out at Shanxi Supercomputing Center of China, and the calculations were performed on TianHe-2.

References

[1] Ashcroft N W 2004 *Phys. Rev. Lett.* **92** 187002
[2] Gao G, Oganov A R, Bergara A *et al.* 2008 *Phys. Rev. Lett.* **101** 107002
[3] Kim D Y, Scheicher R H, and Ahuja R 2009 *Phys. Rev. Lett.* **103** 077002
[4] Drozdov A, Eremets M, Troyan I, Ksenofontov V, and Shylin S 2015 *Nature* **525** 73
[5] Li X F and Peng F 2017 *Lnorg. Chem.* **56** 13759
[6] Liu H Y, Naumov I I, Hoffmann R, Ashcroft N W, and Hemley R J 2017 *Proc. Natl. Acad. Sci. USA* **114** 6990
[7] Somayazulu M, Ahart M, Mishra A K *et al.* 2019 *Phys. Rev. Lett.* **122** 027001

[8] Drozdov A P, Kong P P, Minkov V S *et al.* 2019 *Nature* **569** 528

[9] Hao S, Zhang Z H, Cui T, Pickard C J, Kresin V Z, and Duan D F 2021 *Chin. Phys. Lett.* **38** 107401

[10] Peng F, Sun Y, Pickard C J *et al.* 2017 *Phys. Rev. Lett.* **119** 107001

[11] Sun Y, Lv J, Xie Y, Liu H, and Ma Y 2019 *Phys. Rev. Lett.* **123** 097001

[12] Yang L, Peng S M, Long X G *et al.* 2010 *J. Appl. Phys.* **107** 054903

[13] Wixom R R, Browning J F, Snow C S, Schultz P, and Jennison D R 2008 *J. Appl. Phys.* **103** 123708

[14] Bonnet J and Daou J 1977 *J. Appl. Phys.* **48** 964

[15] Hou P G, Tian F B, Li D *et al.* 2014 *J. Chem. Phys.* **141** 054703

[16] Kuzovnikov M A, Eremets M I, Drozdov A P, and Tkacz M 2017 *Solid State Commun.* **263** 23

[17] Gegenwart P, Si Q, and Steglich F 2008 *Nat. Phys.* **4** 186

[18] Ikeda H, Suzuki M T, and Arita R 2015 *Phys. Rev. Lett.* **114** 147003

[19] Nakai Y, Iye T, Kitagawa S *et al.* 2013 *Phys. Rev. B* **87** 174507

[20] Pines D 2013 *J. Phys. Chem. B* **117** 13145

[21] Tôru M and Kazuo U 2003 *Rep. Prog. Phys.* **66** 1299

[22] Anisimov V I, Zaanen J, and Andersen O K 1991 *Phys. Rev. B* **44** 943

[23] Dudarev S L, Botton G A, Savrasov S Y, Humphreys C J, and Sutton A P 1998 *Phys. Rev. B* **57** 1505

[24] Cococcioni M and de Gironcoli S 2005 *Phys. Rev. B* **71** 035105

[25] Si Q M and Paschen S 2013 *Phys. Status Solidi B* **250** 425

[26] Segall M, Lindan Philip J D, Probert M J *et al.* 2002 *J. Phys.: Condens. Matter* **14** 2717

[27] Perdew J P, Chevary J A, Vosko S H *et al.* 1992 *Phys. Rev. B* **46** 6671

[28] Xu H X, Lee D, Sinnott S B *et al.* 2009 *Phys. Rev. B* **80** 144104

[29] Montanari B and Harrison N M 2002 *Chem. Phys. Lett.* **364** 528

[30] Vajda P and Daou J 1994 *Phys. Rev. B* **49** 3275

[31] Biasini M, Ferro G, Kontrym-Sznajd G, and Czopnik A 2002 *Phys. Rev. B* **66** 075126

[32] Kittel C 1996 *Introduction to Solid State Physics* (New Jersey: John Wiley & Sons Inc.)

[33] Hoshino S and Kuramoto Y 2013 *Phys. Rev. Lett.* **111** 026401

[34] Baroni S, de Gironcoli S, Dal C A, and Giannozzi P 2001 *Rev. Mod. Phys.* **73** 515

[35] Settai R, Takeuchi T, and Ōnuki Y 2007 *J. Phys. Soc. Jpn.* **76** 051003

[36] Kittaka S, Aoki Y, Shimura Y *et al.* 2014 *Phys. Rev. Lett.* **112** 067002

[37] Zhou Y, Wu Q, Rosa Priscila F S *et al.* 2017 *Sci. Bull.* **62** 1439

[38] See Supplemental Material for supporting information of the hypotheses of superconductivity of ErH_2 at 15 and 20 GPa.

[39] Feng D and Jin G J 2012 *Condensed Matter Physics* (Beijing: Higher Education Press) vol 1 pp 503–524 (in Chinese)

[40] Subedi A, Zhang L, Singh D J, and Du M H 2008 *Phys. Rev. B* **78** 134514

[41] Chen G F, Li Z, Wu D *et al.* 2008 *Phys. Rev. Lett.* **100** 247002

[42] Sun H H, Zhang K W, Hu L H *et al.* 2016 *Phys. Rev. Lett.* **116** 257003

[43] Ran S, Eckberg C, Ding Q P *et al.* 2019 *Science* **365** 684

Supplemental Material for

Predicted High-Temperature Superconductivity in Rare Earth Hydride ErH_2 at Moderate Pressure

Yiding Liu(刘一丁),[1,2] Qiang Fan(范强),[3] Jianhui Yang(杨建会),[1] Lili Wang(王丽丽),[4] Weibin Zhang(张伟斌),[5] and Gang Yao(姚钢)[6,7]*

[1]*College of Mathematics and Physics, Leshan Normal University, Leshan 614004, China*

[2] *Institute of Atomic and Molecular Physics, Sichuan University, Chengdu 610065, China*

[3]*School of New Energy Materials and Chemistry, Leshan Normal University, Leshan 614004, China*

[4]*Institute of Computer Application, China Academy of Engineering Physics, Mianyang 621900, China*

[5]*College of Physics and Electronics Information, Yunnan Key Laboratory of Optoelectronic Information Technology, Yunnan Normal University, Kunming, 650500, China*

[6]*School of Physical Science and Technology, Southwest University, Chongqing 400715, China*

[7]*Tsung-Dao Lee Institute, Shanghai Jiao Tong University, Shanghai 200240, China*

*E-mail: yaogang@swu.edu.cn

Table S1. The calculated elastic constants C_{ij} of ErH_2 under ambient pressures (in GPa) and the satisfaction with mechanical stability criteria (Y and N denote the satisfaction and the unsatisfaction, respectively).

P	C_{11}	C_{12}	C_{44}	Y/N
0	121.637	51.209	64.972	Y
6	158.495	59.177	54.465	Y
12	133.738	108.377	113.144	Y
14	145.060	101.757	253.158	Y
14.5	127.776	161.299	192.400	N
15	164.900	103.873	119.387	Y
16	148.068	126.347	76.245	N
18	176.988	105.421	-50.332	N
20	129.393	192.898	-24.491	N

The accompanying behaviors which could also to some extent support the affirmation of superconductivity at 15 GPa are presented in this Supplementary Materials. The calculated elastic constants C_{ij} under ambient pressures are presented in Table S1. Judged from the mechanical stability criterion,[1] this bulk became mechanical unstable at 14.5 GPa and up to 21.5 GPa except 15 GPa, as shown in Table S1. When the applied pressure was higher than 21.5 GPa, this bulk became lattice dynamical unstable, *i.e.*, imaginary frequency of phonon dispersions (not show) which is also the reason why the upper limit of the applied pressure in this work is 21.5 GPa. The mechanical stability criterion for cubic crystal could be expressed as:[1] $\tilde{C}_{44} > 0$, $\tilde{C}_{11} > |\tilde{C}_{12}|$, $\tilde{C}_{11} + 2\tilde{C}_{12} > 0$, where $\tilde{C}_{\alpha\alpha} = C_{\alpha\alpha} - P$ ($\alpha = 1, 4$) and $\tilde{C}_{12} = C_{12} + P$, where P was the applied pressure. Meanwhile, superconductivity could also be reflected by an anomalous elastic softening over a temperature range for $PuCoGa_5$ which was a heavy fermion superconductor with T_c = 18.5 K.[2] Then, the analogous hopping of mechanical stability between 14.5 and 15 GPa of ErH_2 (Table S1) could also support the deduction of superconductivity at 15 GPa.

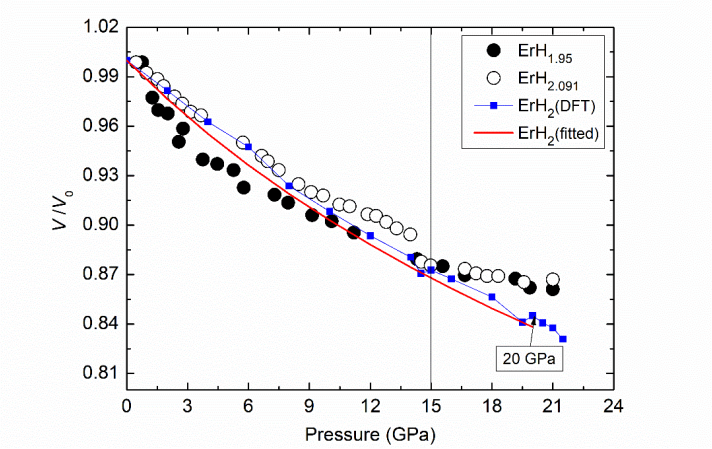

Fig. S1. The fitted normalized molar volumes (V/V_0) as a function of pressures for ErH_2 at 300 K (red solid line) using GIBBS thermodynamics scheme [3] with *E*-*V* data of DFT in this work. The corresponding relation calculated directly with DFT of this work is also plotted (blue solid line with square). The DAC data from Ref. [4] measured at room temperature for $ErH_{1.95}$ (solid circle) and $ErH_{2.091}$ (hollow circle) are also shown for comparison.

By means of Birch–Murnaghan Equation of State (EOS) fitting, the normalized molar volume (V/V_0) of ErH_2 at 300 K as a function of pressures (Fig. S1) is obtained by GIBBS thermodynamics scheme [3] using single point energy of unit cell (E) versus its volume (V) within DFT, *i.e.*, *E*-*V* curve which could be produced in this work (Fig. S2). The corresponding V/V_0 versus pressures relation calculated directly with DFT of this work is also plotted in Fig. S1. There is a tiny and clear deviation at this pressure away from the monotonous trend of the fitted curve in this work. Both the *E*-*V* data and the V/V_0 versus pressures relation of DFT have the same parameter settings and precision with the geometry optimizations of its unit cell (see the main text). The comparison with available experimental data for $ErH_{2.091}$ and $ErH_{1.95}$ measured at room temperature using diamond anvil cell techniques (DAC) [4] is also shown (Fig. S1)

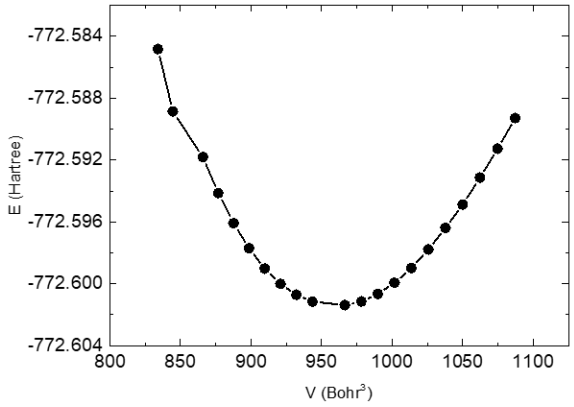

Fig. S2. The single point energy for unit cell (E) of ErH_2 versus its volume (V) within DFT.

The hypothesis of superconductivity at 20 GPa could also be supported by the tiny and clear deviation of the V/V_0 versus pressures relation calculated directly with DFT at this pressure away from the monotonous trend of the curve fitted with E-V data of this work (Fig. S2).

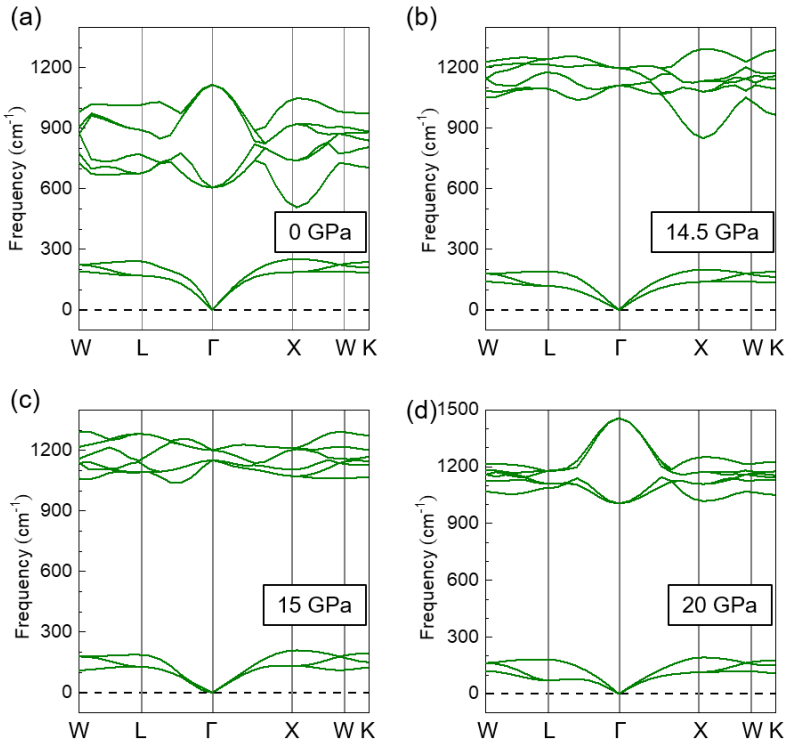

Fig. S3. The calculated phonon dispersions for ErH_2 at (a) 0, (b) 14.5, (c) 15, and (d) 20 GPa.

References

[1] Sin'Ko G and Smirnov N 2002. *J Phys Condens Matter* **14** 6989

[2] Ramshaw B, Shekhter A, McDonald R D, Betts J B, Mitchell J, Tobash P, Mielke C, Bauer E and Migliori A 2015. *Proc. Natl. Acad. Sci. U.S.A.* **112** 3285

[3] Blanco M, Francisco E and Luana V 2004. *Comput. Phys. Commun.* **158** 57

[4] Palasyuk T, Tkacz M and Vajda P 2005. *Solid. State. Commun.* **135** 226